



Characterization of the Differential Pathogenicity of *Candida auris* in a *Galleria mellonella* Infection Model

 Victor Garcia-Bustos,^{a,b,c} Amparo Ruiz-Saurí,^c Alba Ruiz-Gaitán,^b Ignacio Antonio Sigona-Giangreco,^{b,d} Marta Dafne Cabañero-Navalon,^a Oihana Sabalza-Baztán,^d Miguel Salavert-Lletí,^{a,b} María Ángeles Tormo,^b  Javier Pemán^{b,d}

^aDepartment of Internal Medicine and Infectious Diseases, University and Polytechnic La Fe Hospital, Valencia, Spain

^bSevere Infection Research Group, Health Research Institute La Fe, Valencia, Spain

^cDepartment of Pathology, Faculty of Medicine and Dentistry, University of Valencia, Valencia, Spain

^dDepartment of Medical Microbiology, University and Polytechnic La Fe Hospital, Valencia, Spain

ABSTRACT *Candida auris* is an emergent multidrug-resistant fungal pathogen considered a severe global threat due to its capacity to cause nosocomial outbreaks and deep-seated infections with high transmissibility and mortality. However, evidence on its pathogenicity and the complex host-pathogen interactions is still limited. This study used the *in vivo* invertebrate model in *Galleria mellonella* to assess its virulence, exploring the mortality kinetics, melanization response, and morphological changes after fungal infection compared to *Candida albicans* and *Candida parapsilosis*, with known high and low pathogenicity, respectively. All *C. auris* isolates presented less virulence than *C. albicans* strains but higher than that induced by *C. parapsilosis* isolates. Increased pathogenicity was observed in nonaggregative phenotypes of *C. auris*, while the melanization response of the larvae to fungal infection was homogeneous and independent of the causing species. *C. auris* was able to filament in the *in vivo* animal model *G. mellonella*, with aggregative and nonaggregative phenotypes presenting various pseudohyphal formation degrees as pathogenicity determinants in a strain-dependent manner. Histological invasiveness of *C. auris* mimicked that observed for *C. albicans*, with effective dissemination since the early stages of infection both in yeast and filamented forms, except for a remarkable respiratory tropism not previously observed in other yeasts. These characteristics widely differ between strains and advocate the hypothesis that the morphogenetic variability of *C. auris* is an indicator of its flexibility and adaptability, contributing to its emergence and rising worldwide prevalence.

IMPORTANCE *Candida auris* is an emergent fungus that has become a global threat due to its multidrug resistance, mortality, and transmissibility. These unique features make it different from other *Candida* species, but we still do not fully know the degree of virulence and, especially, the host-pathogen interactions. In this *in vivo* insect model, we found that it presents an intermediate degree of virulence compared to known high- and low-virulence *Candida* species but with significant variability between aggregative and nonaggregative strains. Although it was previously considered unable to filament, we documented *in vivo* filamentation as an important pathogenic determinant. We also found that it is able to disseminate early through the host, invading both the circulatory system and many different tissues with a remarkable respiratory tropism not previously described for other yeasts. Our study provides new insights into the pathogenicity of an emergent fungal pathogen and its interaction with the host and supports the hypothesis that its morphogenetic variability contributes to its rising global prevalence.

KEYWORDS *Candida*, *Candida auris*, filamentation, pathogenicity, virulence

Citation Garcia-Bustos V, Ruiz-Saurí A, Ruiz-Gaitán A, Sigona-Giangreco IA, Cabañero-Navalon MD, Sabalza-Baztán O, Salavert-Lletí M, Tormo MÁ, Pemán J. 2021. Characterization of the differential pathogenicity of *Candida auris* in a *Galleria mellonella* infection model. *Microbiol Spectr* 9:e00013-21. <https://doi.org/10.1128/Spectrum.00013-21>.

Editor Christina A. Cuomo, Broad Institute

Copyright © 2021 Garcia-Bustos et al. This is an open-access article distributed under the terms of the [Creative Commons Attribution 4.0 International license](https://creativecommons.org/licenses/by/4.0/).

Address correspondence to Victor Garcia-Bustos, victorgarciabustos@gmail.com.

Received 20 April 2021

Accepted 20 April 2021

Published 9 June 2021

Since the first description of *Candida auris*, its incidence has dramatically risen, causing severe outbreaks of health care-related invasive infections with a high mortality rate (1–4). *C. auris* is noticeably different from most other *Candida* species, owing to its high resistance to antifungal agents and common disinfectants (5, 6), its unprecedented capacity to colonize patients long term and propagate in health care facilities (3, 7), its ability to survive for weeks on fomites and surfaces (1, 8), and the difficulties in its identification by phenotypical and biochemical methods (9). Furthermore, its emergence has been independent and simultaneous on several continents, including Africa, America, Asia, and Europe. Phylogenetic analyses have defined five major clades to date, wherein isolates clustered geographically and appeared nearly identical (2, 10, 11). Although the scientific community has devoted efforts to exploring the biological traits of this unique emergent fungus, there is still limited evidence of its pathogenicity and, especially, the complex host-pathogen interactions. Recently, *Galleria mellonella* has emerged as an alternative to conventional murine models for virulence studies, as its innate immune system at its cellular and humoral level is structurally and functionally similar to that of mammals (12, 13). Besides, the replicability of the model, favored by the possibility to use large numbers of larvae and its lesser ethical implications, has made *G. mellonella* a useful tool to study *Candida* species pathogenicity. Lately, several studies in this model have been performed to assess the virulence of *C. auris* infection (14–17).

Candida albicans is considered the most virulent species of the genus (13, 18), and, among other mechanisms, such as biofilm formation, filamentation is one of its main pathogenicity determinants. Although *C. auris* is thought to be able to form only rudimentary pseudohyphae, especially under stress circumstances (19, 20), some works with a relatively large number of strains have demonstrated a degree of virulence comparable to or even higher than that observed for *C. albicans* (14, 15). The presence of aggregative and nonaggregative phenotypes or even strains with different behaviors, as well as diversity in the expression of proteins related to biofilm formation, filamentation, and other virulence factors (14, 21–23), suggest heterogeneous pathogenicity. Aside from that, the *in vivo* host-pathogen interactions through the histopathological assessment of infected individuals are hardly known, both in animal models and humans.

This study aimed to evaluate the pathogenicity of *C. auris* strains isolated from clinical samples from a large Spanish hospital outbreak in the *G. mellonella* model compared to *C. albicans* and *Candida parapsilosis*, species with known high and low virulence, respectively. This was performed through the analysis of the mortality rate in survival assays and melanization assays and by histopathological assessment of the tissue invasion, host immune response, and fungal distribution *in vivo*.

RESULTS

The characteristics of the 10 isolates of *C. auris* used in this study are presented in Table 1. All strains had been obtained from clinical samples, isolated both from blood cultures of medical and surgical critically ill patients with invasive infection and from cultures of epidemiological surveillance. In a previous work of our group (7), we analyzed 58 *C. auris* isolates (41 blood isolates and 17 epidemiological surveillance isolates) from 48 patients using the amplified fragment length polymorphism (AFLP) technique. The results suggested that our isolates are clonal, with an overall similarity of >96%. In addition, our isolates form a separate and distinct group, both from isolates from other countries and from phylogenetically close yeasts, and are only related to isolates from South Africa (clade III). These results were further confirmed by whole-genome sequencing (WGS) at the Mycology Reference Lab of the Carlos III Institute and by Chow et al. (10). The cj98 strain used in this work was sequenced in those works. Hence, our strains were assumed to belong to clade III. Clinical isolates from patients with invasive disease were tested for antifungal susceptibility. All were fluconazole

TABLE 1 Characteristics of the *C. auris* strains used in this study^a

Strain	Origin	Patient diagnosis	Department	Phenotype	MIC (mg/liter)									
					AMB	5FC	FLU	ITR	VOR	CAS	ANI	MCF	POS	ISA
Cj98	Blood	Polytrauma	SICU	Nonaggregative	0.25	0.12	>256	0.25	2	0.5	0.06	0.06	0.03	0.064
Cj104	Blood	Polytrauma	SICU	Aggregative	0.5	0.06	>256	0.125	2	0.03	0.125	0.06	0.06	NA
Cj173	Blood	Polytrauma	SICU	Aggregative	0.5	<0.06	>256	0.06	2	0.06	0.06	0.06	0.03	NA
Cj175	Blood	Status epilepticus	MICU	Nonaggregative	0.5	0.06	>256	0.125	2	0.03	0.125	0.06	0.06	NA
Cj197	Blood	Febrile neutropenia	Medicine	Nonaggregative	2	0.25	>256	0.25	4	0.5	0.5	0.25	0.06	0.064
Cj198	Blood	Pneumonia	MICU	Aggregative	0.25	0.06	>256	0.25	1	0.06	0.125	0.06	0.03	NA
312775	Blood	Endocarditis	MICU	Nonaggregative	0.5	0.06	>256	0.125	8	0.03	0.125	0.06	0.06	0.75
124819	Rectal	Respiratory failure + ECMO	MICU	Nonaggregative	0.5	<0.06	>256	0.06	0.03	0.03	0.06	0.03	0.015	0.25
182482	Inguinal	Liver Tx	MICU	Nonaggregative	0.5	<0.06	>256	0.06	0.03	0.03	0.03	0.03	0.015	0.5
253107	Pharyngeal	Multiple myeloma	MICU	Nonaggregative	0.5	<0.06	>256	0.06	0.03	0.03	0.125	0.03	0.015	0.25

^aECMO, extracorporeal membrane oxygenation; Tx, transplant; NA, not applicable.

resistant and echinocandin susceptible. *C. auris* strain Cj197 was considered resistant to amphotericin B by following the CDC tentative breakpoints (24).

***Galleria mellonella* survival assays. (i) *C. auris* presents an intermediate degree of virulence between *C. albicans* and *C. parapsilosis*.** Globally, significant differences were observed in the survival profile of *G. mellonella* larvae infected with *C. albicans*, *C. auris*, and *C. parapsilosis* species ($P < 0.0001$). The median survival was 48 h for *C. auris* and *C. parapsilosis* and 24 h for *C. albicans*, as seen in Fig. 1A. Larvae inoculated with *C. albicans* strains displayed significantly higher mortality rates than those infected with both *C. auris* ($P = 0.00012$) and *C. parapsilosis* ($P < 0.0001$). Moreover, *C. auris* strains showed higher virulence and produced lower survival rates than *C. parapsilosis* strains ($P = 0.018$). In all experiments, no larval deaths were documented in control groups inoculated with phosphate-buffered saline (PBS). The survival rates at half the observation time (120 h) were 6% (95% confidence interval [CI], 2.8 to 10.9) for *C. auris*, 2.9% (95% CI, 0.5 to 8.9) for *C. albicans*, and 15.6% (95% CI, 8.6 to 24.5) for *C. parapsilosis*. The Kaplan-Meier survival plots are represented in Fig. 1.

(ii) Aggregative *C. auris* isolates are less pathogenic than nonaggregative isolates. Aggregative and nonaggregative *C. auris* phenotypes were compared. While both presented a median survival of 48 h in infected larvae, nonaggregative *C. auris* strains were significantly more pathogenic than phenotypically aggregative strains ($P = 0.0194$) (Fig. 1B). The survival rates at half the observation time of aggregative and nonaggregative strains were 12.5% (95% CI, 4.6 to 24.6) and 3.2% (95% CI, 0.9 to 9.3), respectively. Both phenotypes were also differentially compared with *C. albicans* and *C. parapsilosis*. Nonaggregative strains exhibited significantly greater virulence than *C. parapsilosis* strains ($P = 0.006$) but still lower than that observed in larvae infected with *C. albicans* ($P = 0.010$), as also observed with aggregative strains ($P = 0.00046$).

(iii) Clinical origin or drug resistance is not associated with increased virulence in *C. auris*. No statistically significant differences were observed in the mortality induced by the amphotericin B-resistant *C. auris* strain Cj197, even after stratification by phenotype ($P = 0.578$). *C. auris* strains isolated from clinical samples of patients with invasive disease were not significantly more virulent than those obtained from epidemiological surveillance cultures, as represented in Fig. 1C ($P = 0.172$).

G. mellonella larvae did not show statistically significant differences in survival profiles in the penalized pairwise analysis, depending on each of the 10 individual isolates of *C. auris* they were infected with ($P = 0.134$), despite some interstrain variability. All *C. auris* strains induced significantly higher mortality rates than the negative control ($P < 0.0001$). The individual strains that seemed to be less virulent coincided with aggregative phenotypes (strains Cj104, Cj173, and Cj198). Similarly, no statistically significant differences were observed in the mortality rate after infection with the strains of *C. albicans* ($P = 0.347$). Wider differences could be observed in the interstrain pathogenicity of the other isolates of *C. parapsilosis*, although these were not statistically significant in our work either ($P = 0.0678$). All strains from both species were significantly

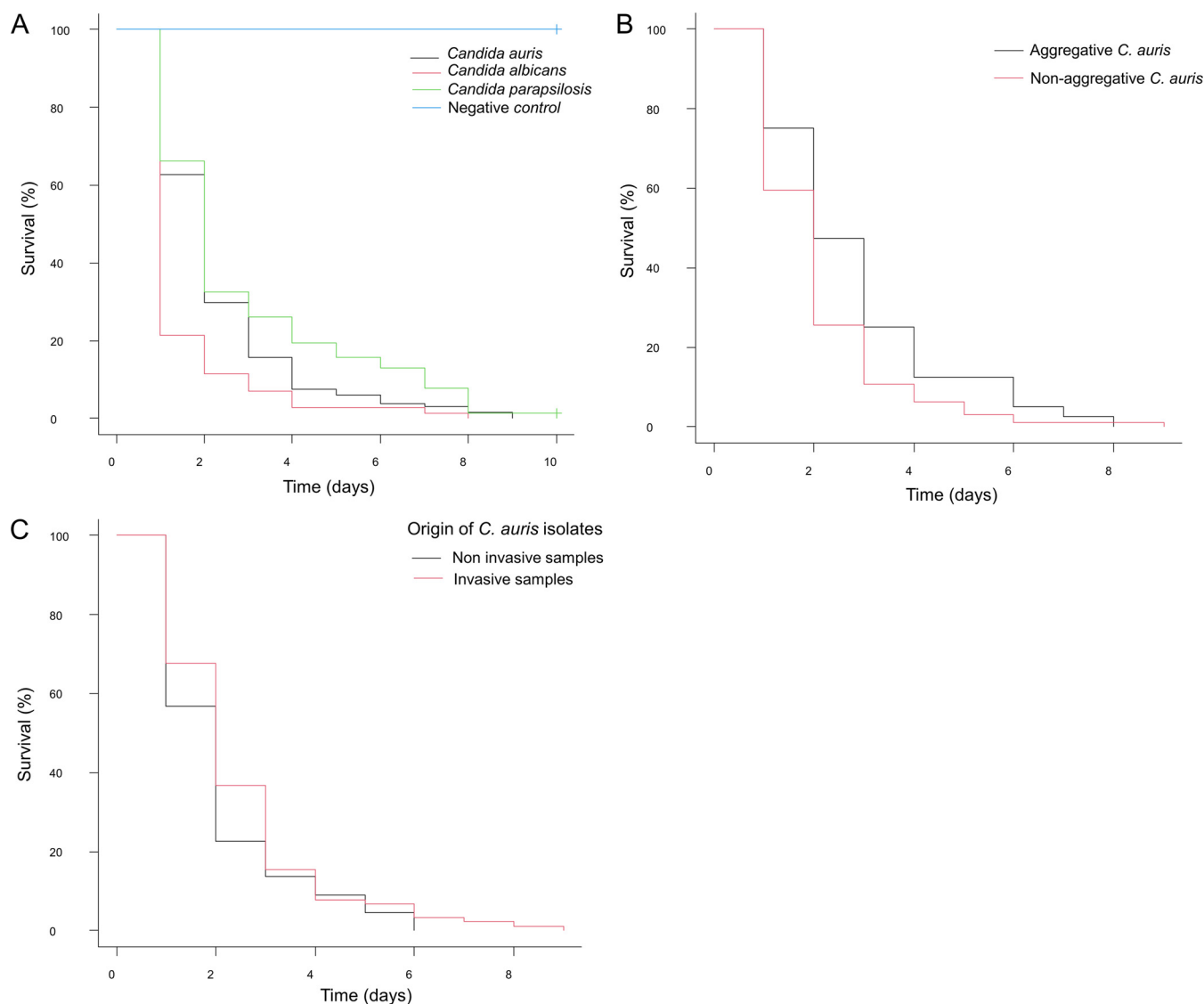


FIG 1 Kaplan-Meier survival curves of *G. mellonella* after infection with different *Candida* species. (A) Differences in global mortality kinetics between *C. auris* (2018-1-124819, Cj104, Cj98, 253107, 182482, 312755, Cj197, Cj198, Cj175, and Cj173), *C. albicans* (255083, Ca591, Ca581, Ca550, and Ca560), and *C. parapsilosis* (22019, 6308, Cp661, Cp664, Cp665, Cp669, Cp672, and Cp673) strains, including the negative control. (B) Differences in survival after infection with *C. auris* aggregative (Cj104, Cj173, and Cj198) and nonaggregative (2018-1-124819, Cj98, 253107, 182482, 312755, Cj175, and Cj197) phenotypes. (C) Differences in survival after infection with *C. auris* strains isolated from invasive samples (Cj98, Cj104, Cj173, Cj175, Cj197, Cj198, and 312775) and noninvasive samples (cultures of epidemiological surveillance) (124819, 182482, and 253107). All strains of different species, *C. auris* phenotypes, and clinical origins of *C. auris* were jointly assessed in the global analysis. Individual strain curves and data can be seen in the supplemental material.

virulent compared to the negative control ($P < 0.0001$). The survival Kaplan-Meier curves of all strains and nonstatistically significant comparisons can be found in the supplemental material.

Melanization assays show the melanization response of *G. mellonella* to fungal infection seems to be independent of the infecting species. The degree of larval melanization was studied as a response to *Candida* species infection. In all three species, the melanization response in *G. mellonella* followed a logarithmic regression curve. The trend lines of the evolution of the mean larval melanization considering all strains of *C. auris*, *C. albicans*, and *C. parapsilosis* are represented in Fig. 2. No statistically significant differences were observed, as all three species induced similar melanization responses. However, as seen in Fig. 2, *C. albicans* strains seemed to cause the overall higher melanization rates, followed by *C. auris* and *C. parapsilosis* strains. Day four was chosen as the closer time to the inflection point of the curve. At this point,

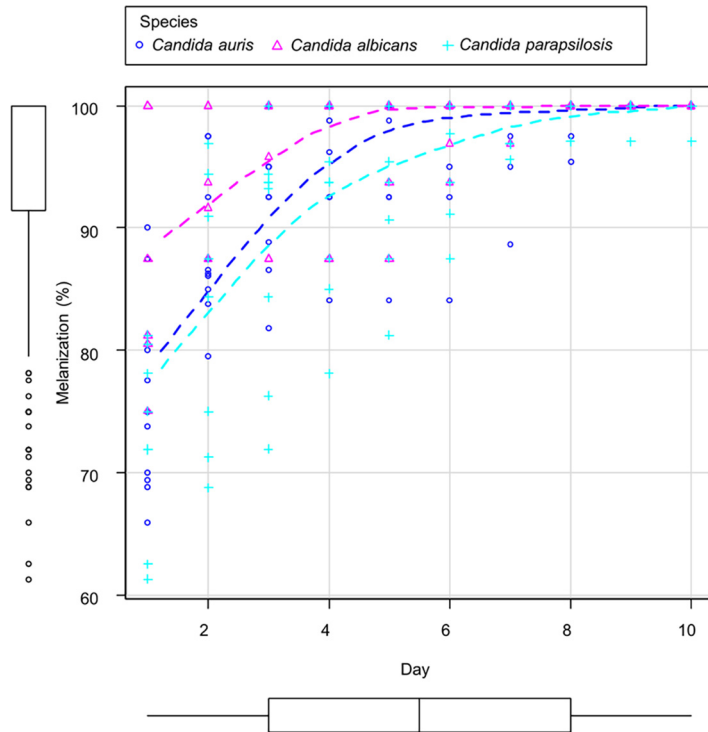


FIG 2 Scatterplot summarizing the melanization response of *G. mellonella* larvae after infection with different *Candida* species. The scatterplot represents the global mean percentage of larval melanization of each group of 10 larvae per strain for each day during the observation period, grouped by the different species. Smooth fitted lines are depicted for each species. All strains of the study were included in the analysis.

the mean degree of melanization in *C. auris* was 96.41% (standard deviations [SD], 5.29) in *C. albicans* was 95.54% (SD, 5.94) and in *C. parapsilosis* was 92.05% (SD, 8.77). To highlight, the reference *C. albicans* strains SC5314 and Ca550 induced severe and rapid melanization of up to 100% at 24 h. The nonaggregative *C. auris* strains Cj198 (87.5% at 24 h) and Cj175 (90% at 24 h) owned their group's higher melanization rates.

Histopathology of infection in *G. mellonella*. (i) Fungal invasiveness, distribution, filamentation, and immune response after *G. mellonella* infection with *C. auris*. The fungal distribution, morphology, and burden was studied using periodic acid-Schiff (PAS), and the immune response was assessed with hematoxylin-eosin (H-E). In the *C. auris* infection model, significant dissemination was observed 24 h after inoculation, especially in nonaggregative strains. Mainly hemolymphatic dissemination was seen during these earlier stages, following a wider distribution throughout the tissue with a notable peritracheal involvement (Fig. 3A). *In vivo* infection induced pseudohypha formation in *C. auris*, mainly observed in hemolymph but also invading tissue and within granuloma-like formations (Fig. 3A to C). Various degrees of filamentation were observed in all strains, both in aggregative and nonaggregative phenotypes. Some strains, such as Cj175 or 253107, showed frequent and defined pseudohyphae, while in other isolates, such as Cj101, only rudimentary forms were observed. Large yeast aggregates with biofilm appearance were observed, especially in nonaggregative strains, within larger areas of disrupted and necrotic tissue with lower inflammatory response and with a time-dependent abundance (Fig. 3D). Increased numbers of activated hemocytes were seen in the inoculum site at 24 h. Hemocytes were later activated and recruited through various tissues; fewer subcuticular immature cells were observed, and activated histiocytic-like spindle cells were visualized in the fat body, digestive, and respiratory structures in later phases of the infection in surviving larvae (Fig. 4B to D). Significantly, hemocytes nodules, some containing fungal elements and

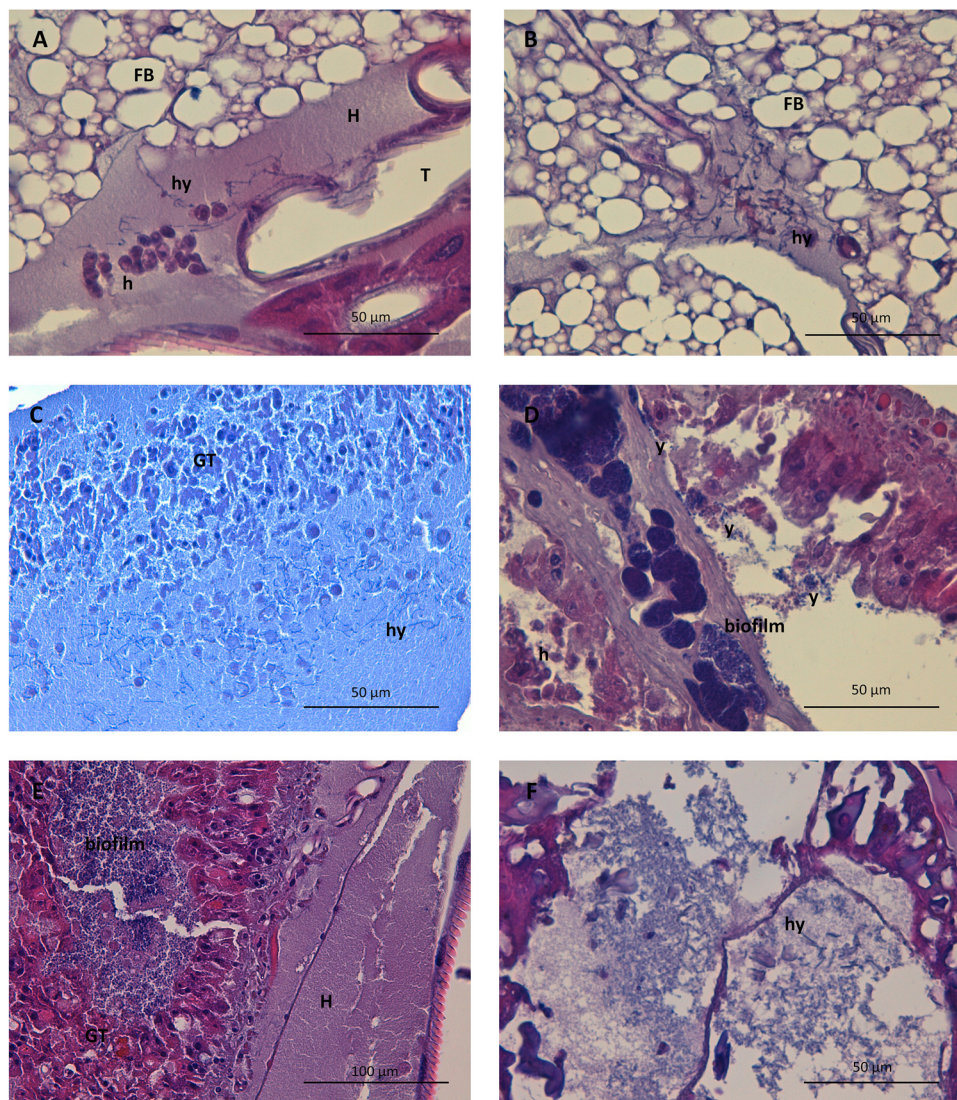


FIG 3 Representative photomicrographs of the fungal morphology and distribution in the *G. mellonella* model after infection with *C. auris*, *C. albicans*, and *C. parapsilosis* at different times. (A) Filamented *C. auris* disseminating through the hemolymph and invading the insect respiratory system twenty-four hours after infection with strain 253107. Periodic acid-Schiff (PAS) staining was used at $\times 630$ magnification. (B) Invasion of the fat body by pseudohyphae of *C. auris* 24 h after infection with strain 253107. PAS staining is shown at $\times 630$ magnification. (C) Pseudohyphae and yeasts of *C. auris* within the large granuloma-like formation of activated hemocytes of distinct lineages 48 h after infection with strain Cj175. Hematoxylin-eosin (H-E) staining is shown at $\times 630$ magnification. (D) Large nodules of *C. auris* with yeast morphology and biofilm appearance within a matrix of detritus and inflammatory cells 24 h after infection with strain 253107. PAS staining is shown at $\times 630$ magnification. (E) Granuloma-like formation with abundant necrosis surrounding significant accumulations of yeasts of *C. albicans* 48 h after infection with strain 255083. PAS staining is shown at $\times 400$ magnification. (F) Yeast and filamented forms of *C. parapsilosis* 120 h after infection with strain 2209. PAS staining is shown at $\times 630$ magnification. Abbreviations: FB, fat body; GT, granulation-like tissue; H, hemolymph; h, hemocytes; hy, pseudohyphae; T, tracheal system; y, yeasts.

melanin deposits, were formed dispersed in the fat body, frequently surrounding tracheae, but also intestinal walls and, in some cases, even muscular tissue (Fig. 4B to D). Even in the early stages, granuloma-like formations containing yeasts and pseudohyphae were found (Fig. 4E). Melanization bodies were subjectively larger and more frequent after infection by aggregative *C. auris* strains.

(ii) Fungal invasiveness, distribution, filamentation and immune response after *G. mellonella* infection with *C. albicans* and *C. parapsilosis*. *C. albicans* produced a faster and more aggressive progression of infection. Even in the earlier phases, the

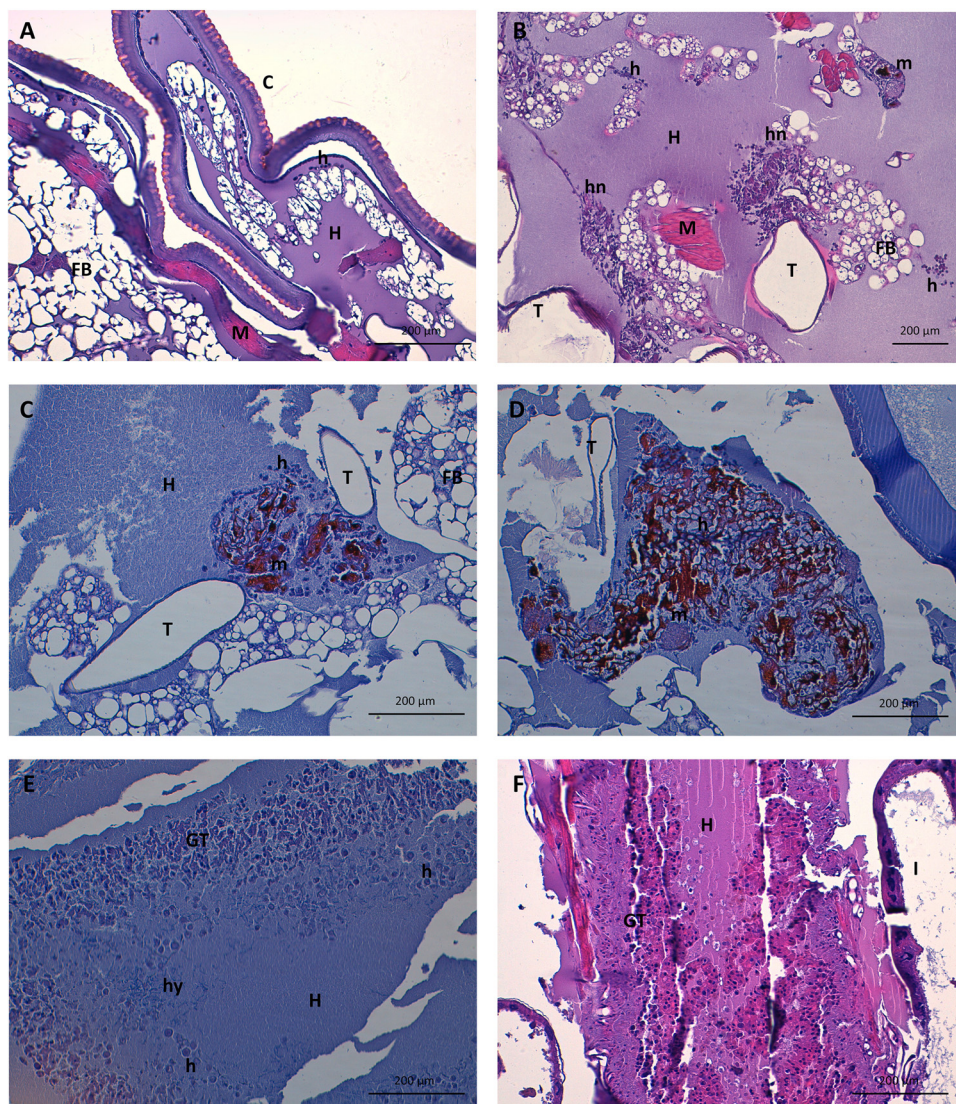


FIG 4 Histological response to fungal infection after inoculation of 10^6 CFU/larvae of *Candida auris*. (A) Negative control. Note several isolated subcuticular hemocytes and conserved tissue architecture. Hematoxylin-eosin (H-E) staining is shown at $\times 200$ magnification. (B) Inflammatory infiltrate conforming hemocyte nodules with peritracheal distribution of *C. auris* 48 h after infection with strain Cj104. H-E staining is shown at $\times 100$ magnification. (C) Hemocyte nodule containing melanin deposits and possibly yeasts and pseudohyphae of *C. auris* with both peritracheal and hemolymphatic distribution 48 h after infection with strain Cj101. H-E staining is shown at $\times 100$ magnification. (D) Large hemocyte nodule with abundant melanin deposits and fungal elements within after infection by *C. auris* at 48 h after infection with strain 175. H-E staining is shown at $\times 200$ magnification. (E) Granulomatous tissue formed by activated hemocytes of different lineages and filamented structures of *C. auris* 48 h after infection with strain Cj175. H-E staining is shown at $\times 200$ magnification. (F) Advanced stage of the infection by *C. auris*, with significant tissue destruction and necrosis and inflammatory response with granulation-like tissue 120 h after infection with strain Cj104. H-E staining is shown at $\times 200$ magnification. Abbreviations: C, cuticle; FB, fat body; GT, granulation-like tissue; I, intestinal tract; T, tracheal system; H, hemolymph; h, hemocyte; hn, hemocyte nodule; hy, pseudohyphae; M, muscle; m, melanin; y, yeasts.

fungal elements reach solid organs, with significant tropism for the digestive tract. The infection also appears highly destructive and induced an intense inflammatory and even desmoplastic response, with granulation tissue containing highly abundant fungal elements with biofilm appearance (Fig. 3E). Forty-eight hours postinoculation, large amounts of fungal elements, both in yeast and filamented forms, distribute widely through the tissue, even distally to the inoculation point. In some strains, such as SC5314, marked filamentation is observed.

In the infection model with *C. parapsilosis*, both tissue invasion and inflammatory response are subjectively lower than that in larvae infected with *C. auris* and *C. albicans*, even in surviving larvae up to 120 h postinfection. Lesser solid-organ invasion is seen, and frequent fungal elements are seen in subcuticular regions and fat bodies. Granuloma-like formations were isolated and smaller than those observed in *C. auris* and *C. albicans*. Pseudohyphal forms were also found (Fig. 3F).

DISCUSSION

The main findings can be summarized as follows. (i) *C. auris* isolates were less virulent than *C. albicans* strains but more virulent than *C. parapsilosis* isolates. (ii) Aggregative phenotypes of *C. auris* were less pathogenic than nonaggregative ones. (iii) *C. auris*, *C. albicans*, and *C. parapsilosis* induced similar rates of macroscopic melanization as a response to infection. (iv) *C. auris* can filament in the *in vivo* *G. mellonella* animal model. Both aggregative and nonaggregative phenotypes present pseudohyphal formation as pathogenicity mechanisms. (v) High tissue invasiveness is a general characteristic of *C. auris*. It mimics *C. albicans* but presents a general peritracheal distribution not previously described, inducing large granuloma-like formations and traveling both in yeast and filamented forms through liquid and solid compartments.

Since the discovery of *C. auris* (4), some works have been devoted to identifying its virulence and pathogenic mechanisms at both cellular and molecular levels due to its particular properties that are rarely observed in other yeasts (14–17), but the data are still limited and highly diverse. The understanding of its pathogenesis depends upon the highly complex host-pathogen interactions. The animal model *G. mellonella* is a useful tool for studying *Candida* species pathogenicity due to its high degree of structural and functional similarity with the innate immune system of mammals and has fewer ethical constraints (13, 25–29).

C. auris not only differs greatly from other species but also exhibits significant intraspecies heterogeneity, which evidences the need to include as many strains as possible as well as strains belonging to the different known clades (30–32). Therefore, to date, the degree of pathogenicity of *C. auris* compared to other *Candida* species is still under discussion. Moreover, the amount of *in vivo* studies and the number of strains used in the literature is still improvable. Furthermore, some studies present methodological limitations that constrain their external validity.

Borman and colleagues (14) used a relatively large number of United Kingdom isolates (12) and demonstrated strain-specific differences in *C. auris* pathogenicity. As in our study, aggregative phenotypes were less virulent than nonaggregative ones, as described previously (15). However, in contrast to our findings, the pathogenicity of nonaggregative isolates was similar to that observed in *C. albicans*. Nevertheless, despite the fact that Kaplan-Meier plots were created, the use of the Mann-Whitney test in larva survival comparison is debatable, and no *P* value penalization was applied in multiple comparisons, exponentially raising the probability of type 1 error. No histological assessment and no *in vivo* host-yeast interaction studies were performed. However, the global survival curves of *C. auris* in *G. mellonella* in their work are somehow similar to those obtained in our assays. Hence, despite there being statistically significant differences, its biological implications are unclear. Moreover, the use of this model serves as an initial approximation of the pathogenicity of *C. auris* in higher animals, but the validation of results will require further confirmatory mammalian testing. Strikingly, in the work by Sherry and coworkers (15) using 4 UK strains of *C. auris*, the *C. auris* strain SC5314 and *C. glabrata* WT2001, *C. albicans* and nonaggregating phenotypes of *C. auris* had similar kill kinetics with an inoculum of 10^6 CFU, and the mortality induced by *C. auris* was even higher than that of *C. albicans* with a lower inoculum of 10^5 CFU.

On the contrary, we reported lower mortality rates in larvae infected with *C. auris* than with *C. albicans*, in line with other studies, both in the different individual strains and phenotypes (16, 17). On the one hand, in experiments by Muñoz et al., the

pathogenicity of 5 Colombian strains of *C. auris* was compared with the reference *C. albicans* strain SC5314 in the *G. mellonella* model and with the reference *C. albicans* strain ATCC 10231 in an immunosuppressed murine model as well as with strains of the *C. haemulonii* complex. Their findings in the *G. mellonella* model regarding their lower pathogenicity species control (*C. haemulonii* complex) are similar to ours concerning *C. parapsilosis*: in their study, *C. auris* strains showed significantly higher virulence than *C. haemulonii* complex species and lower pathogenicity than *C. auris* SC5314. In our work, significantly lower pathogenicity was observed in all strains of *C. parapsilosis* compared to *C. albicans*, as widely known (33), as well as *C. auris*. However, these results were not replicated in their murine model. Similar to previous evidence (15), a significantly higher capability of biofilm formation was seen in *C. auris* compared to the *C. haemulonii* species complex, and a higher fungal burden was also reported for *C. auris*. No distinction was made in this work between aggregative and nonaggregative phenotypes.

On the other hand, Romera et al. (16) used three Spanish strains of both *C. auris* and *C. albicans*, and an assessment of melanization, cocoon formation, and larva activity was also performed. However, no histological analyses were performed to corroborate results with findings regarding fungal morphology and behavior *in vivo* as well as the host immune system-yeast interactions. While their findings concur with our evidence regarding higher virulence observed in *C. albicans*, related to lower larval activity and cocoon formation but maintaining similar melanization levels, as in our case, no differences were observed in aggregative and nonaggregative phenotypes. Additionally, significant differences between clinical and reference strains were found in both species, probably owing to variations of the expression of virulence factors (16, 34, 35). In our work, despite all strains of *C. auris* being clinical, no differences were found in kill kinetics between strains isolated from invasive samples or cultures of epidemiological surveillance. This suggests that virtually all strains have the potential to provoke severe invasive disease independently of their isolation, as has been shown previously (27, 36).

Beyond the stated limitations of previous works and their mainly exploratory nature due to a lack of histological assessment and use of a small number of strains, the significant virulence heterogeneity between clades, phenotypes, and strains seems evident (32) and has been observed in other *Candida* species (33). *C. auris* has unique characteristics that make it different from other known yeasts and facilitate host infection and high environmental adaptation, and various virulence factors have been described to date. These variations in their pathogenicity determinants derived from the genomic plasticity of *C. auris* may explain this intraspecies heterogeneity.

Filamentation and biofilm formation, phenotypic switching, metabolic flexibility and pH adaptation, production of extracellular hydrolytic and cytolytic proteins, secretion of heat shock proteins, and adherence mechanisms are some of the major virulence determinants of *Candida* species (37, 38). Little is still known about *C. auris* virulence factors. Biofilm formation and hyphal growth have been considered the core factors enhancing the progression of pathogenicity in *Candida* spp. (37). Different authors have previously underlined the inability of *C. auris* to produce pseudohyphae both *in vitro* and in several models of infection, including *G. mellonella*, mouse, and human (1, 14, 17, 32, 39). This fact is distinctive, especially considering that filamentation has been linked to invasive ability into host tissues (40), and the lethality of invasive infections is up to 60% (2, 36, 41). However, it is evident that many other factors, such as diagnostic delay, multidrug resistance, or comorbidities, among others, are directly related to poorer outcomes in infected patients. Surprisingly, we have noted *in vivo* significant but divergent filamentation in both aggregative and nonaggregative phenotypes, ranging from rudimentary to well-defined pseudohyphae. These structures have been observed traveling free through the hemolymph, which raises the theory that dissemination to different organs through the circulatory system depends on normal yeast cells (20). Unlike *C. albicans*, which presents important gastrointestinal

tropism in the *G. mellonella* model (25), pseudohyphae have been observed invading tissue with a remarkable peritracheal involvement in all strains of *C. auris* from both clinical invasive and epidemiological surveillance samples, which is not previously described in the literature for other yeasts, and within granuloma-like formations of spindle cells and activated hemocytes. However, this information is qualitative, and further quantitative or semiquantitative approaches must be performed to confirm this hypothesis in the insect model. Besides, insect models only represent the innate immune system and give no insight on the adaptive immune mechanisms of mammals. Insect larvae lack many of the target organs of invasive fungal infections, and these data should be further replicated, at least in murine models. Recently, some studies have also reported filamentation in strains of *C. auris* under particular conditions or stress. Yue et al. described a heritable phenotypic switch to filamentation-competent/filamentous phenotype triggered by passage through the mammalian body and temperature changes. Bravo Ruiz and coworkers (19) were able to induce filamentation *in vitro* triggered by genotoxic stress. Remarkably, and in line with our work, Sherry et al. (15) described pseudohyphae in *C. auris* biofilms and Fan et al. (42) reported filamentation in strains of four major clades, both in the *G. mellonella* model. The fact that in some works no expression of hyphae-related proteins, such as candidalysin (ECE1) or hyphal cell wall protein (HWP1), has been detected (23), and that *C. auris* strains have differential biofilm-forming capability (15) or diversity in the expression of other virulence factors also seen in *C. albicans* (21, 22), suggests that the remarkable morphogenetic plasticity of *C. auris* is an indicator of its flexibility and adaptability and could contribute to its emergence and rising worldwide prevalence. Moreover, it questions the idea that each clade harbors nearly identical strains and emphasizes the importance of transcriptomic and proteomic analyses of different strains (2, 43, 44).

Our study presents several important limitations that need to be acknowledged. This is probably the most extensive study analyzing *C. auris* pathogenicity in terms of survival, melanization, and host-yeast histological interactions. However, the number of tested strains is relatively low and research is still needed, including more isolates of different morphologies, phenotypes, and clades due to the heterogeneous nature of the species. Our histological approach was qualitative, and larger and, more importantly, quantitative morphometric studies are needed to corroborate the results and analyze the immune response and fungal burden and distribution *in vivo*. Furthermore, other markers, such as larval activity and cocoon formation, have been described during the realization of this work. Genomic, proteomic, hemocyte count, and biofilm capacity analyses were not performed and are of interest in the study of fungal pathogenicity, especially in the unique context of *C. auris*.

In conclusion, *G. mellonella* is a useful model to evaluate the pathogenicity of emerging fungal pathogens such as *C. auris*. The virulence features of *C. auris* observed in this study widely differ between strains and clades. Further studies on pathogenicity mechanisms *in vitro* and *in vivo* are needed to keep unraveling the pathogenicity of this intriguing species.

MATERIALS AND METHODS

Fungal strains. Ten strains of *C. auris* (2018-1-124819, Cj104, Cj98, 253107, 182482, 312755, Cj197, Cj198, Cj175, and Cj173), isolated both from blood cultures and epidemiological surveillance cultures of patients admitted to the University and Polytechnic Hospital La Fe (UPHLF), were selected in a randomized manner from the strain collection database of our institution.

The BacT/Alert Virtuo automated system (bioMérieux, Marcy l'Etoile, France) was used to process blood cultures. *C. auris* identification was performed in the Department of Microbiology of the UPHLF by sequencing the internal transcribed spacer (ITS) using the primers ITS3-ITS4 and ITS2-ITS5 with the GenomeLab™ GeXP system (Beckman Coulter, Fullerton, CA, USA). It was later confirmed in the Spanish Mycology Reference Laboratory using ITS1-ITS4 primers. Phenotypic classification of *C. auris* strains into aggregative and nonaggregative phenotypes was carried out by vigorous vortexing for 3 min with 1 ml of sterile saline containing a concentration of 10^8 CFU/ml and immediate direct view of $10\ \mu\text{l}$ of the solution at $\times 200$ magnification using a TC20 automated cell counter (Bio-Rad Laboratories, France).

For the higher pathogenicity control model, six strains of *C. albicans* were chosen. Five (255083,

Ca591, Ca581, Ca550, and Ca560) were obtained from blood cultures of patients from the UPHLF. One was isolated from cerebrospinal fluid (CSF) (Ca589), and one was the reference strain SC5314. For the lower pathogenicity control model, eight strains of *C. parapsilosis* (22019, 6308, Cp661, Cp664, Cp665, Cp669, Cp672, and Cp673), isolated from blood cultures of patients from the UPHLF, were used. Clinical isolates of *C. albicans* and *C. parapsilosis* species were identified in the Department of Microbiology of the UPHLF by using the matrix-assisted laser desorption ionization time of flight Vitek mass spectrometry system (bioMérieux, France). *In vitro* antifungal susceptibility was determined by EUCAST methodology. MIC was defined as the concentration achieving 50% growth inhibition after 24 h of incubation at 35°C (90% in the case of amphotericin B). MIC was determined by the colorimetric microdilution panel Sensititre YeastOne Y010 (TREK Diagnostic Systems, Oakwood Village, OH) according to the manufacturer's instructions. The MIC to isavuconazole was determined by Etest isavuconazole Liofilchem MTS (Liofilchem, Roseto degli Abruzzi, Italy). CDC tentative breakpoints were applied for *C. auris* MIC interpretation (24).

All strains were kept at -80°C until use.

***Galleria mellonella*.** Sixth-instar larvae of *G. mellonella* were acquired from the genome-sequenced breeding stock TruLarv (BioSystems Technology Ltd., UK). Nonmelanized active larvae weighing 250 to 350 mg were selected, and a first decontamination using 70% ethanol was carried out. Groups of 10 larvae were then placed in petri dishes and maintained at 15°C under dark conditions until inoculation.

Survival assays in *G. mellonella*. Survival assays in *G. mellonella* were performed by following previous protocols (14). Suspensions of *Candida* species isolates were grown on Sabouraud's agar for 24 h at 37°C. Colonies were collected with sterile plastic loops, washed twice in sterile PBS, counted with a TC20 automated cell counter (Bio-Rad Laboratories, France), and adjusted to 10^5 CFU/ μl in sterile PBS. As Borman et al. (14) described, the obtaining of inocula of *C. auris* aggregate strains was performed by acquiring homogeneous suspensions by allowing initial suspensions to settle for 10 min, removing the supernatant containing individual yeasts, and then adjusting the concentration to 10^5 CFU/ μl . Before inoculation, larvae were further decontaminated with 70% ethanol. Individual larvae were infected by intrahemocoelic injection of 10 μl of the solution (10^6 CFU) in the left rear proleg using a 10- μl Hamilton syringe with a 26-gauge blunt needle. A minimum of 10 larvae per isolate were used in the cases of *C. albicans* and *C. parapsilosis*, and a minimum of 20 larvae per isolate were used in the cases of *C. auris*. Negative controls with sterile PBS were performed in the same way using groups of 10 larvae. Infected larvae were placed in petri dishes in groups of 10 and incubated at 37°C. Every petri dish was tagged with an individual code to blind the further scoring. Deaths and cocoons that occurred in the first 12 h after inoculation were discarded. Death of larvae was scored daily for 10 days.

Melanization assays in *G. mellonella*. The degree of melanization of the infected larvae in the survival assays was also monitored daily during the 10-day follow-up period. In each experiment, the percentage of body melanization was noted from 0 to 100% per larva and per day. The dead larvae were also recorded, scoring 100%. All processes were also blindly registered.

Histopathology of *G. mellonella*. Surviving larvae infected with each of the three species of *Candida* were euthanized after 24 h, 48 h, and 120 h. Euthanasia was performed in a 2-step method by following the AVMA guidelines for the euthanasia of animals (45). Larvae were first anesthetized through immersion in 5% ethanol and later euthanized by immersion in a solution of neutral-buffered 10% formalin to preserve tissue anatomy and start fixation. To perform an adequate fixation and maximum tissue preservation, larvae were maintained in this solution for 3 to 4 weeks to allow cuticular penetration and tissue diffusion. After fixation, they were sagittally sectioned and embedded in paraffin for processing. Conventional hematoxylin-eosin (H-E) staining was performed for the larvae's anatomical assessment and the immune response to infection. Periodic acid-Schiff staining (PAS) was performed to evaluate the fungal morphology and distribution, and Grocott-Gomori's methenamine silver stain was performed to confirm fungal morphology. Uninfected larvae were equally processed for comparative purposes. Histological samples were analyzed with a Leica DMD108 optic light microscope (Leica Microsystems, Wetzlar, Germany), and photomicrographs were taken at different magnifications.

Statistical analysis. The statistical analysis was performed with R statistical package version 4.0.3. (R Development Core Team, 2020). In the survival assays, Kaplan-Meier survival curves were created, and the log-rank test was used to compare larva survival in different groups. A *P* value of <0.05 was considered statistically significant. The Bonferroni adjustment method was applied for pairwise comparison. For the global comparison between species, all larvae from all strains of each species were included in the analysis, and the same methodology was performed depending on the grouping variables.

For the analysis of melanization assays, the mean degree of melanization for each observation day was calculated per strain and per experiment. A grouped scatterplot representing the global mean percentage of larval melanization of each group of 10 larvae per strain for each day during the observation period, grouped by the different species, was created, and smooth fitted lines were depicted. Day four after the infection was chosen according to the designed curves to analyze melanization rates. Normality was assessed using quantile-quantile plots, and the Kruskal-Wallis test by ranks was used.

The data set can be found in the Figshare repository with https://figshare.com/articles/dataset/Pathogenicity_auris_DB/14222456.

Ethics statement. The study protocol was approved by the Research Commission and the Scientific and Ethical Committees of the Health Research Institute La Fe with registry code 2017-0682. As the study was conducted in fungal strains and insect larvae and all clinical information of the origin of the samples was anonymous, no evaluation by the Institutional Animal Care Committee or informed consents were required.

SUPPLEMENTAL MATERIAL

Supplemental material is available online only.

SUPPLEMENTAL FILE 1, PDF file, 1.2 MB.

REFERENCES

- Ruiz-Gaitan A, Martinez H, Moret AM, Calabuig E, Tasiás M, Alastruey-Izquierdo A, Zaragoza O, Mollar J, Frasquet J, Salavert-Lleti M, Ramirez P, Lopez-Hontangas JL, Peman J. 2019. Detection and treatment of *Candida auris* in an outbreak situation: risk factors for developing colonization and candidemia by this new species in critically ill patients. *Expert Rev Anti Infect Ther* 17:295–305. <https://doi.org/10.1080/14787210.2019.1592675>.
- Lockhart SR, Etienne KA, Vallabhaneni S, Farooqi J, Chowdhary A, Govender NP, Colombo AL, Calvo B, Cuomo CA, Desjardins CA, Berkow EL, Castanheira M, Magobo RE, Jabeen K, Asghar RJ, Meis JF, Jackson B, Chiller T, Litvintseva AP. 2017. Simultaneous emergence of multidrug-resistant *Candida auris* on 3 continents confirmed by whole-genome sequencing and epidemiological analyses. *Clin Infect Dis* 64:134–140. <https://doi.org/10.1093/cid/ciw691>.
- Eyre DW, Sheppard AE, Madder H, Moir I, Moroney R, Quan TP, Griffiths D, George S, Butcher L, Morgan M, Newnham R, Sunderland M, Clarke T, Foster D, Hoffman P, Borman AM, Johnson EM, Moore G, Brown CS, Walker AS, Peto TEA, Crook DW, Jeffery KJM. 2018. A *Candida auris* outbreak and its control in an intensive care setting. *N Engl J Med* 379:1322–1331. <https://doi.org/10.1056/NEJMoa1714373>.
- Satoh K, Makimura K, Hasumi Y, Nishiyama Y, Uchida K, Yamaguchi H. 2009. *Candida auris* sp. nov., a novel ascomycetous yeast isolated from the external ear canal of an inpatient in a Japanese hospital. *Microbiol Immunol* 53:41–44. <https://doi.org/10.1111/j.1348-0421.2008.00083.x>.
- Chowdhary A, Sharma C, Meis JF. 2017. *Candida auris*: a rapidly emerging cause of hospital-acquired multidrug-resistant fungal infections globally. *PLoS Pathog* 13:e1006290. <https://doi.org/10.1371/journal.ppat.1006290>.
- Ku TSN, Walraven CJ, Lee SA. 2018. *Candida auris*: disinfectants and implications for infection control. *Front Microbiol* 9:726. <https://doi.org/10.3389/fmicb.2018.00726>.
- Ruiz-Gaitan A, Moret AM, Tasiás-Pitarch M, Aleixandre-Lopez AI, Martinez-Morel H, Calabuig E, Salavert-Lleti M, Ramirez P, Lopez-Hontangas JL, Hagen F, Meis JF, Mollar-Maseres J, Peman J. 2018. An outbreak due to *Candida auris* with prolonged colonisation and candidaemia in a tertiary care European hospital. *Mycoses* 61:498–505. <https://doi.org/10.1111/myc.12781>.
- Welsh RM, Bentz ML, Shams A, Houston H, Lyons A, Rose LJ, Litvintseva AP. 2017. Survival, persistence, and isolation of the emerging multidrug-resistant pathogenic yeast *Candida auris* on a plastic health care surface. *J Clin Microbiol* 55:2996–3005. <https://doi.org/10.1128/JCM.00921-17>.
- Iguchi S, Itakura Y, Yoshida A, Kamada K, Mizushima R, Arai Y, Uzawa Y, Kikuchi K. 2019. *Candida auris*: a pathogen difficult to identify, treat, and eradicate and its characteristics in Japanese strains. *J Infect Chemother* 25:743–749. <https://doi.org/10.1016/j.jiac.2019.05.034>.
- Chow NA, Munoz JF, Gade L, Berkow EL, Li X, Welsh RM, Forsberg K, Lockhart SR, Adam R, Alanio A, Alastruey-Izquierdo A, Althawadi S, Arauz AB, Ben-Ami R, Bharat A, Calvo B, Desnos-Ollivier M, Escandon P, Gardam AB, Gunturu R, Heath CH, Kurzai O, Martin R, Litvintseva AP, Cuomo CA. 2020. Tracing the evolutionary history and global expansion of *Candida auris* using population genomic analyses. *mBio* 11:e03364-19. <https://doi.org/10.1128/mBio.03364-19>.
- Chow NA, de Groot T, Badali H, Abastabar M, Chiller TM, Meis JF. 2019. Potential fifth clade of *Candida auris*, Iran, 2018. *Emerg Infect Dis* 25:1780–1781. <https://doi.org/10.3201/eid2509.190686>.
- Brennan M, Thomas DY, Whiteway M, Kavanagh K. 2002. Correlation between virulence of *Candida albicans* mutants in mice and *Galleria mellonella* larvae. *FEMS Immunol Med Microbiol* 34:153–157. <https://doi.org/10.1111/j.1574-695X.2002.tb00617.x>.
- Borman AM. 2018. Of mice and men and larvae: *Galleria mellonella* to model the early host-pathogen interactions after fungal infection. *Virulence* 9:9–12. <https://doi.org/10.1080/21505594.2017.1382799>.
- Borman AM, Szekely A, Johnson EM. 2016. Comparative pathogenicity of united kingdom isolates of the emerging pathogen *Candida auris* and other key pathogenic *Candida* species. *mSphere* 1:e00189-16. <https://doi.org/10.1128/mSphere.00189-16>.
- Sherry L, Ramage G, Kean R, Borman A, Johnson EM, Richardson MD, Rautemaa-Richardson R. 2017. Biofilm-forming capability of highly virulent, multidrug-resistant *Candida auris*. *Emerg Infect Dis* 23:328–331. <https://doi.org/10.3201/eid2302.161320>.
- Romera D, Aguilera-Correa JJ, Garcia-Coca M, Mahillo-Fernandez I, Vinuela-Sandoval L, Garcia-Rodriguez J, Esteban J. 2020. The *Galleria mellonella* infection model as a system to investigate the virulence of *Candida auris* strains. *Pathog Dis* 78:ftaa067. <https://doi.org/10.1093/femspd/ftaa067>.
- Munoz JE, Ramirez LM, Dias LDS, Rivas LA, Ramos LS, Santos ALS, Taborda CP, Parra-Giraldo CM. 2020. Pathogenicity levels of colombian strains of *Candida auris* and Brazilian strains of *Candida haemulonii* species complex in both murine and *Galleria mellonella* experimental models. *J Fungi* 6:104. <https://doi.org/10.3390/jof6030104>.
- Hirayama T, Miyazaki T, Ito Y, Wakayama M, Shibuya K, Yamashita K, Takazono T, Saijo T, Shimamura S, Yamamoto K, Imamura Y, Izumikawa K, Yanagihara K, Kohno S, Mukae H. 2020. Virulence assessment of six major pathogenic *Candida* species in the mouse model of invasive candidiasis caused by fungal translocation. *Sci Rep* 10:3814. <https://doi.org/10.1038/s41598-020-60792-y>.
- Bravo Ruiz G, Ross ZK, Gow NAR, Lorenz A. 2020. Pseudohyphal growth of the emerging pathogen *Candida auris* is triggered by genotoxic stress through the S phase checkpoint. *mSphere* 5:e00151-20. <https://doi.org/10.1128/mSphere.00151-20>.
- Yue H, Bing J, Zheng Q, Zhang Y, Hu T, Du H, Wang H, Huang G. 2018. Filamentation in *Candida auris*, an emerging fungal pathogen of humans: passage through the mammalian body induces a heritable phenotypic switch. *Emerg Microbes Infect* 7:188. <https://doi.org/10.1038/s41426-018-0187-x>.
- Alfouzan W, Dhar R, Albarrag A, Al-Abdely H. 2019. The emerging pathogen *Candida auris*: a focus on the Middle-Eastern countries. *J Infect Public Health* 12:451–459. <https://doi.org/10.1016/j.jiph.2019.03.009>.
- Larkin E, Hager C, Chandra J, Mukherjee PK, Retuerto M, Salem I, Long L, Isham N, Kovanda L, Borroto-Esoda K, Wring S, Angulo D, Ghannoum M. 2017. The emerging pathogen *Candida auris*: growth phenotype, virulence factors, activity of antifungals, and effect of SCY-078, a novel glucan synthesis inhibitor, on growth morphology and biofilm formation. *Antimicrob Agents Chemother* 61:e02396-16. <https://doi.org/10.1128/AAC.02396-16>.
- Munoz JF, Gade L, Chow NA, Loparev VN, Juieng P, Berkow EL, Farrer RA, Litvintseva AP, Cuomo CA. 2018. Genomic insights into multidrug-resistance, mating and virulence in *Candida auris* and related emerging species. *Nat Commun* 9:5346. <https://doi.org/10.1038/s41467-018-07779-6>.
- CDC. 2020. Antifungal susceptibility testing and interpretation. Centers for Disease Control and Prevention, Atlanta, GA. <https://www.cdc.gov/fungal/candida-auris/c-auris-antifungal.html>.
- Perdoni F, Falleni M, Tosi D, Cirasola D, Romagnoli S, Braidotti P, Clementi E, Bulfamante G, Borghi E. 2014. A histological procedure to study fungal infection in the wax moth *Galleria mellonella*. *Eur J Histochem* 58:2428. <https://doi.org/10.4081/ejh.2014.2428>.
- Ames L, Duxbury S, Pawlowska B, Ho HL, Haynes K, Bates S. 2017. *Galleria mellonella* as a host model to study *Candida glabrata* virulence and antifungal efficacy. *Virulence* 8:1909–1917. <https://doi.org/10.1080/21505594.2017.1347744>.
- Frenkel M, Mandelblat M, Alastruey-Izquierdo A, Mendlovic S, Semis R, Segal E. 2016. Pathogenicity of *Candida albicans* isolates from bloodstream and mucosal candidiasis assessed in mice and *Galleria mellonella*. *J Mycol Med* 26:1–8. <https://doi.org/10.1016/j.mycmed.2015.12.006>.
- Gago S, Garcia-Rodas R, Cuesta I, Mellado E, Alastruey-Izquierdo A. 2014. *Candida parapsilosis*, *Candida orthopsilosis*, and *Candida metapsilosis* virulence in the non-conventional host *Galleria mellonella*. *Virulence* 5:278–285. <https://doi.org/10.4161/viru.26973>.
- Mesa-Arango AC, Forastiero A, Bernal-Martinez L, Cuenca-Estrella M, Mellado E, Zaragoza O. 2013. The non-mammalian host *Galleria mellonella* can be used to study the virulence of the fungal pathogen *Candida tropicalis* and the efficacy of antifungal drugs during infection by this

- pathogenic yeast. *Med Mycol* 51:461–472. <https://doi.org/10.3109/13693786.2012.737031>.
30. Rhodes J, Fisher MC. 2019. Global epidemiology of emerging *Candida auris*. *Curr Opin Microbiol* 52:84–89. <https://doi.org/10.1016/j.mib.2019.05.008>.
 31. Chybowska AD, Childers DS, Farrer RA. 2020. Nine things genomics can tell us about *Candida auris*. *Front Genet* 11:351. <https://doi.org/10.3389/fgene.2020.00351>.
 32. Forgacs L, Borman AM, Prepost E, Toth Z, Kardos G, Kovacs R, Szekely A, Nagy F, Kovacs I, Majoros L. 2020. Comparison of in vivo pathogenicity of four *Candida auris* clades in a neutropenic bloodstream infection murine model. *Emerg Microbes Infect* 9:1160–1169. <https://doi.org/10.1080/22221751.2020.1771218>.
 33. Marcos-Zambrano LJ, Bordallo-Cardona MA, Borghi E, Falleni M, Tosi D, Munoz P, Escribano P, Guinea J. 2020. *Candida* isolates causing candidemia show different degrees of virulence in *Galleria mellonella*. *Med Mycol* 58:83–92. <https://doi.org/10.1093/mmy/myz027>.
 34. Monroy-Perez E, Paniagua-Contreras GL, Rodriguez-Purata P, Vaca-Paniagua F, Vazquez-Villasenor M, Diaz-Velasquez C, Uribe-Garcia A, Vaca S. 2016. High virulence and antifungal resistance in clinical strains of *Candida albicans*. *Can J Infect Dis Med Microbiol* 2016:5930489. <https://doi.org/10.1155/2016/5930489>.
 35. Romera D, Aguilera-Correa JJ, Gadea I, Vinuela-Sandoval L, Garcia-Rodriguez J, Esteban J. 2019. *Candida auris*: a comparison between planktonic and bio-film susceptibility to antifungal drugs. *J Med Microbiol* 68:1353–1358. <https://doi.org/10.1099/jmm.0.001036>.
 36. Garcia-Bustos V, Salavert M, Ruiz-Gaitan AC, Cabanero-Navalon MD, Sigona-Giangreco IA, Peman J. 2020. A clinical predictive model of candidaemia by *Candida auris* in previously colonized critically ill patients. *Clin Microbiol Infect* 26:1507–1513. <https://doi.org/10.1016/j.cmi.2020.02.001>.
 37. Mba IE, Nweze EI. 2020. Mechanism of *Candida* pathogenesis: revisiting the vital drivers. *Eur J Clin Microbiol Infect Dis* 39:1797–1819. <https://doi.org/10.1007/s10096-020-03912-w>.
 38. Staniszewska M. 2020. Virulence factors in *Candida* species. *Curr Protein Pept Sci* 21:313–323. <https://doi.org/10.2174/1389203720666190722152415>.
 39. Azar MM, Turbett SE, Fishman JA, Pierce VM. 2017. Donor-derived transmission of *Candida auris* during lung transplantation. *Clin Infect Dis* 65:1040–1042. <https://doi.org/10.1093/cid/cix460>.
 40. Brand A. 2012. Hyphal growth in human fungal pathogens and its role in virulence. *Int J Microbiol* 2012:517529. <https://doi.org/10.1155/2012/517529>.
 41. Schelenz S, Hagen F, Rhodes JL, Abdolrasouli A, Chowdhary A, Hall A, Ryan L, Shackleton J, Trimlett R, Meis JF, Armstrong-James D, Fisher MC. 2016. First hospital outbreak of the globally emerging *Candida auris* in a European hospital. *Antimicrob Resist Infect Control* 5:35. <https://doi.org/10.1186/s13756-016-0132-5>.
 42. Fan S, Yue H, Zheng Q, Bing J, Tian S, Chen J, Ennis CL, Nobile CJ, Huang G, Du H. 2021. Filamentous growth is a general feature of *Candida auris* clinical isolates. *Med Mycol*. <https://doi.org/10.1093/mmy/myaa116>.
 43. Chow NA, Gade L, Tsay SV, Forsberg K, Greenko JA, Southwick KL, Barrett PM, Kerins JL, Lockhart SR, Chiller TM, Litvintseva AP, US *Candida auris* Investigation Team. 2018. Multiple introductions and subsequent transmission of multidrug-resistant *Candida auris* in the USA: a molecular epidemiological survey. *Lancet Infect Dis* 18:1377–1384. [https://doi.org/10.1016/S1473-3099\(18\)30597-8](https://doi.org/10.1016/S1473-3099(18)30597-8).
 44. Chatterjee S, Alampalli SV, Nageshan RK, Chettiar ST, Joshi S, Tatu US. 2015. Draft genome of a commonly misdiagnosed multidrug resistant pathogen *Candida auris*. *BMC Genomics* 16:686. <https://doi.org/10.1186/s12864-015-1863-z>.
 45. Leary SU, Anthony R, Cartner S, Grandin T, Greenacre CB, Gwaltney-Bran S, McCrackin MA, Meyer R, Miller D, Shearer J, Turner T, Yanon R. 2020. AVMA guidelines for the euthanasia of animals, 2020 ed. American Veterinary Medical Association, Schaumburg, IL.